SAR Minimum-Entropy Autofocus Using an Adaptive-Order Polynomial Model

Junfeng Wang and Xingzhao Liu

***Abstract*—A new algorithm is presented for autofocus in synthetic aperture radar imaging. Entropy is used to measure the focus quality of the image, and better focus corresponds to smaller entropy. The phase response of the focus filter is modeled as a specially designed polynomial, and the coefficients of this polynomial are adjusted in sequence to minimize the entropy of the image. Because the order of this polynomial is adaptive, this algorithm applies more widely than the minimum-entropy algorithms with a fixed-order polynomial model.**

***Index Terms*—Autofocus, entropy, synthetic aperture radar (SAR).**

I. Introduction

SYNTHETIC aperture radar (SAR) uses the relative motion between the radar and the target to image the target. In different applications, it takes different modes, like stripmap SAR and spotlight SAR. We consider stripmap SAR in this letter. The addressed ideas and methods, however, can be extended into other modes of SAR (such as spotlight SAR) and inverse SAR (ISAR).

There are three typical algorithms for SAR imaging: the range-Doppler algorithm [1], the chirp-scaling algorithm [2], and the wavenumber-domain algorithm [3]. In this letter, we study the range-Doppler algorithm. First, signals from scatterers with different ranges are resolved using their differences in time delay. A wideband technique, like the matched-filter technique, the stretch technique, or the step-chirp technique, is usually used to improve range resolution. Then, the signals from the scatterers with different azimuths are resolved using their differences in slow time. Clutter lock, range correction, and focus are used to improve azimuth resolution.

SAR utilizes a focus filter to obtain a fine azimuth resolution. Usually, the focus filter is designed on the basis that the radar moves regularly and the target is stationary. If the radar moves irregularly, or the target is moving, the focus filter may not focus the signal well, and the image may be blurred. In such cases, the focus filter can be designed based on the signal. This is referred to as autofocus. Typical methods for autofocus include the subaperture-correlation method [1], the phase-gradient method [4], [5], the time-frequency method [6], the phase-difference method [7], and the image-optimization method [8]–[14]. Some of these methods are originally used in spotlight SAR or ISAR. However, they can be extended into stripmap SAR.

Manuscript received November 24, 2005; revised April 11, 2006.

The authors are with the Department of Electronic Engineering, Shanghai Jiaotong University, Shanghai 200030, China (e-mail: junfengwang@sjtu.edu.cn).

Digital Object Identifier 10.1109/LGRS.2006.878446

Image-optimization autofocus has been shown to have good performance [8]–[14]. In this technique, the phase response of the focus filter is designed to optimize the focus quality of the image. The focus quality of the image can be measured by contrast [8], [12]–[14], entropy [9]–[14], or another function [12]. Different measures are preferred in different applications [12].

Image-optimization autofocus is originally implemented by a parametric algorithm [8], [9]. The phase response of the focus filter is represented by a parametric model, and the parameters of this model are selected to optimize the focus quality of the image. However, depending on the relative motion between the radar and the target, the phase response of the focus filter may take any form. If the phase response of the focus filter does not fit the assumed model, the parametric implementation cannot work well. In order to remove this limitation, a nonparametric algorithm is presented to implement image-optimization autofocus [10]. This algorithm does not use any parametric model for the phase response of the focus filter, and thus applies universally. However, since it solves the optimization problem by trial and error, this algorithm is computationally inefficient. In order to raise the computational efficiency, two other nonparametric algorithms, the gradient-search algorithm and the fixed-point algorithm, are proposed to carry out image-optimization autofocus [11]. They are detailed in [12]–[14], respectively. Both algorithms are much more efficient in the computation than the nonparametric algorithm in [10], although they are not as efficient in the computation as the parametric implementation.

We present a new algorithm to implement image-optimization autofocus. Due to its good performance in our previous work, entropy is used to measure the focus quality of the image. Better focus results in smaller entropy. In order to gain high computational efficiency, this algorithm is parametric. The phase response of the focus filter is modeled as a specially designed polynomial, and the coefficients of this polynomial are adjusted in sequence to minimize the entropy of the image. The order of this polynomial is adaptive, and thus, this algorithm applies more widely than the minimum-entropy algorithms with a fixed-order polynomial model. Some results of this letter have been given in [14].

II. Rationale

Target points with different slant ranges have different phase errors. Depending on the relative motion between the radar and the target, the target points with the same slant range but different azimuths may also have different phase errors. Thus, strictly speaking, different target points require different focus

filters. Actually, it almost does not degrade the focus quality of the image to use a single focus filter for a target patch, when the patch has a small size such that its points have similar phase errors. The patch may even be the entire target.

Next, consider the focus of a target patch. This is carried out by a focus filter, i.e.,

$$g(m,n)=\frac{1}{M}\sum_{k=0}^{M-1}F(k,n)\exp\left[j\varphi(k)\right]\exp\left(j\frac{2\pi}{M}km\right). \quad (1)$$

m, n, and k are the indexes in slow time, range, and Doppler frequency, respectively. $F(k,n)$ is the signal to be focused, and $\varphi(k)$ is the phase response of the focus filter. Compared to the phase response, the amplitude response of the focus filter is trivial and is assumed to be unit. $g(m,n)$ is the complex image. The key to autofocus is the estimation of $\varphi(k)$. In the minimum-entropy autofocus, $\varphi(k)$ is designed to minimize the entropy of $|g(m,n)|^2$.

The entropy of $|g(m,n)|^2$ is defined as

$$\varepsilon\left[|g(m,n)|^2\right]=\sum_{m=0}^{M-1}\sum_{n=0}^{N-1}\frac{|g(m,n)|^2}{S}\ln\frac{S}{|g(m,n)|^2} \quad (2)$$

where

$$S=\sum_{m=0}^{M-1}\sum_{n=0}^{N-1}|g(m,n)|^2. \quad (3)$$

Entropy can be used to measure the smoothness of a distribution function. The smoother a distribution function is, the larger the entropy is. In SAR imaging, owing to this property, entropy can be used to measure the focus quality of an image [9]–[14]. Better focus results in a sharper image, and thus smaller entropy. Therefore, in autofocus, the phase response of the focus filter can be designed to minimize the entropy of the image.

Equation (2) is also written as

$$\varepsilon\left[|g(m,n)|^2\right]=\ln S-\frac{1}{S}\sum_{m=0}^{M-1}\sum_{n=0}^{N-1}|g(m,n)|^2\ln|g(m,n)|^2. \quad (4)$$

When the amplitude response of the focus filter is assumed to be a unit, S is a constant, and thus, the entropy can be redefined as

$$\varepsilon'\left[|g(m,n)|^2\right]=-\sum_{m=0}^{M-1}\sum_{n=0}^{N-1}|g(m,n)|^2\ln|g(m,n)|^2. \quad (5)$$

Thus, the minimum-entropy autofocus can be formulated as finding the phase response of the focus filter which minimizes (5).

III. Algorithm

A. Model of $\varphi(k)$

Let ω be the Doppler frequency in radians, and let $\phi(\omega)$ be the phase response of the focus filter in terms of ω. We model

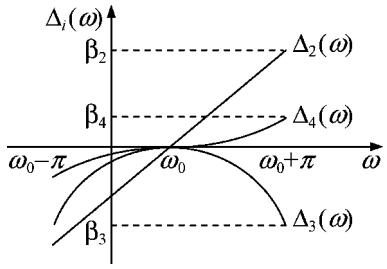

Fig. 1. Illustration of β_i.

$\phi(\omega)$ as a polynomial, i.e.,

$$\phi(\omega)=-\sum_{i=2}^{I}\pi\frac{\beta_i}{i}\left(\frac{\omega-\omega_0}{\pi}\right)^i,\qquad \omega_0-\pi\le\omega<\omega_0+\pi. \quad (6)$$

i begins from 2. Because it has no effect on the entropy of the image, the zeroth-order term is ignored. The first-order term is also ignored, because it has no effect on the entropy of the image either, although it causes a shift of the image in azimuth. I is adaptive and depends on the complexity of $\phi(\omega)$. ω_0 is the Doppler centroid in radians. The focus filter has a group delay of zero at $\omega=\omega_0$ in order to avoid the shift of the image in azimuth. β_i is the parameter to be estimated.

The ith-order term in (6) causes a group delay

$$\Delta_i(\omega)=\beta_i\left(\frac{\omega-\omega_0}{\pi}\right)^{i-1},\qquad \omega_0-\pi<\omega<\omega_0+\pi. \quad (7)$$

$\Delta_i(\omega)$ is actually the time delay of the signal at the instantaneous frequencies ω due to the ith-order term. Letting $\omega\to(\omega_0+\pi)^-$ in (7), we obtain

$$\beta_i=\lim_{\omega\to(\omega_0+\pi)^-}\Delta_i(\omega). \quad (8)$$

That is, β_i is actually the limit of $\Delta_i(\omega)$, as ω approaches $(\omega_0+\pi)^-$ (Fig. 1). It indicates the extent of deblurring achieved by the ith-order term.

The discrete-frequency version of (6) is

$$\varphi(k)=-\sum_{i=2}^{I}\pi\frac{\beta_i}{i}\left[\frac{2}{M}(k-k_0)\right]^i,\qquad k_0-\frac{M}{2}\le k<k_0+\frac{M}{2}. \quad (9)$$

k_0 is the Doppler centroid in the interval of ω, i.e.,

$$k_0=\frac{M}{2\pi}\omega_0. \quad (10)$$

It may not be an integer. In order to utilize the fast Fourier transform and the inverse fast Fourier transform, (9) is written as

$$\varphi(k)=\begin{cases}-\sum_{i=2}^{I}\pi\frac{\beta_i}{i}\left[\frac{2}{M}(k-k_0)\right]^i, & 0\le k<k_0+\frac{M}{2}\\ -\sum_{i=2}^{I}\pi\frac{\beta_i}{i}\left[\frac{2}{M}(k-k_0-M)\right]^i, & k_0+\frac{M}{2}\le k<M.\end{cases} \quad (11)$$

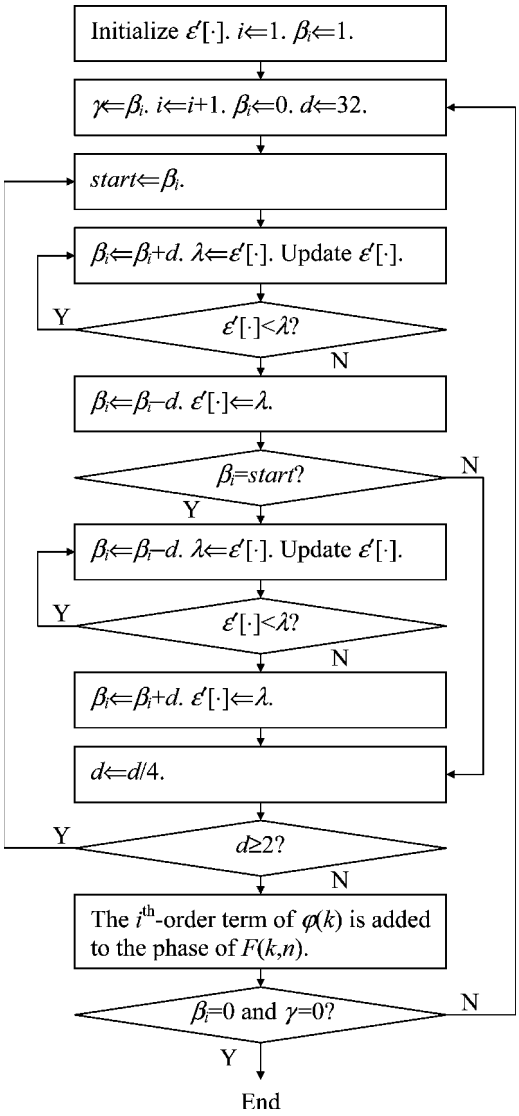

Fig. 2. Estimation of β_i.

k_0 is estimated by clutter lock. Typical methods for clutter lock are summarized in [1], like the nominal-envelope method, the energy-balance method, the maximum-likelihood method, and the time-domain method. When different methods are used, the estimates of k_0 may be different. As a result, the estimates of β_i may also be different. Nevertheless, in our tests, the obtained focus filter can always focus the signal well. We use the nominal-envelope method in Section IV.

B. Estimation of $\varphi(k)$

To improve the computational efficiency, the signal is focused using the regular focus filter before autofocus. The regular focus filter also has a group delay of zero at the Doppler centroid to avoid the shift of the image in azimuth.

β_i is estimated by the algorithm in Fig. 2. First, β_2 is increased step by step until $\varepsilon'[\cdot]$ is minimized. If it cannot be increased by even one step, β_2 is decreased step by step until $\varepsilon'[\cdot]$ is minimized. Then, the above process is repeated for smaller step sizes. Next, β_3, β_4, and so on are adjusted in the same way.

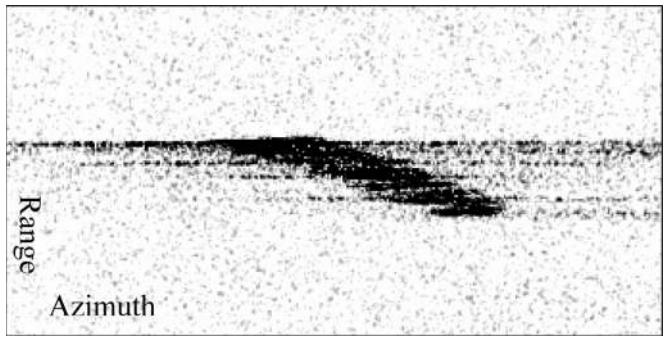

Fig. 3. Image by conventional focus.

Given the same value, different β_i's correspond to comparable amounts of deblurring. Thus, different β_i's can be adjusted using the same step sizes. The minimum step size of β_i should be chosen to achieve a good tradeoff between the estimation accuracy and the computational efficiency. The smaller the minimum step size is, the higher the estimation accuracy is. However, the computational efficiency may be lower, because more steps may be required. In Section IV, the minimum step size of β_i is chosen as 2. The initial step size and the decrease factor of β_i should be chosen to have a small number of steps, and thus a high computational efficiency. Actually, there exists a large freedom in choosing the two parameters. In Section IV, the initial step size of β_i is chosen as 32, and the decrease factor of β_i is chosen as 4.

The order of $\varphi(k)$ is adaptive, and is assumed to be high enough, when the estimates of the two consecutive β_i's are equal to zero. This is justified by our tests. In the tests, we find that with i increasing, the estimate of β_i converges to zero, and when the estimates of the two consecutive β_i's are equal to zero, higher order terms are ignorable basically. Our tests also show that $\varphi(k)$ can be approximated by such a polynomial in general.

IV. Results

The data of a moving boat are used to evaluate our algorithm. The data came from the Danish EMISAR system.

Fig. 3 shows the image obtained by the conventional focus, i.e., the phase response is designed on the basis that the radar moves regularly and the target is stationary. Owing to the motion of the boat, the image is blurred. Fig. 4 shows the image obtained by minimum-entropy autofocus with a fixed-order polynomial model (quadratic). As we see, the image is better focused. Fig. 5 shows the image obtained by the minimum-entropy autofocus with an adaptive-order polynomial model. The obtained phase response is a fifth-order polynomial. We can see that the image is also better focused. For the data, because the phase error is basically quadratic, the two minimum-entropy algorithms have similar performances.

A sinusoidal phase error is added to the Doppler spectra of the original signals, and the simulated data are used to evaluate our algorithm. The sinusoidal phase error is given by

$$\theta(\omega) = 120\sin\left(\frac{\omega-\omega_0}{2}\right), \qquad \omega_0-\pi\leq\omega<\omega_0+\pi. \tag{12}$$

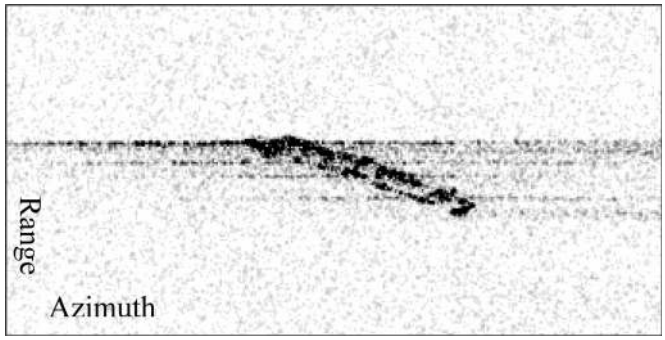

Fig. 4. Image by minimum-entropy autofocus with a fixed-order polynomial model.

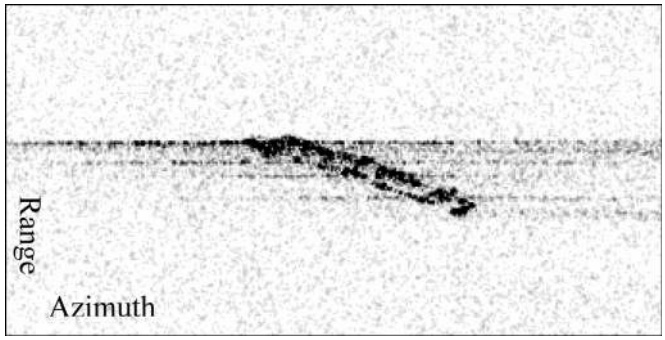

Fig. 5. Image by minimum-entropy autofocus with an adaptive-order polynomial model.

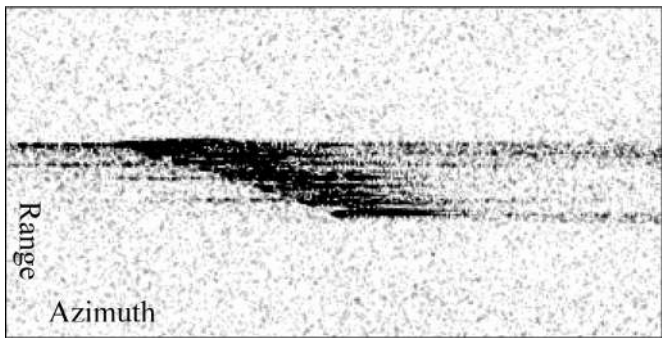

Fig. 6. Image by conventional focus from the simulated data.

Fig. 6 shows the image obtained by the conventional focus. We can see that the image is blurred. Fig. 7 shows the image obtained by the minimum-entropy autofocus with a fixed-order polynomial model. As we see, the image is still blurred. The image in Fig. 8 is obtained by the minimum-entropy autofocus with an adaptive-order polynomial model. The obtained phase response is an eighth-order polynomial. The image is better focused than those in Figs. 6 and 7.

Entropy can be used to measure the focus quality of an image, and better focus results in a smaller entropy. Table I gives the entropies of the images in Figs. 3–8. Here, entropy is calculated by (5). From Table I, we can conclude that the minimum-entropy autofocus with an adaptive-order polynomial model causes better focus than the minimum-entropy autofocus with a fixed-order polynomial model.

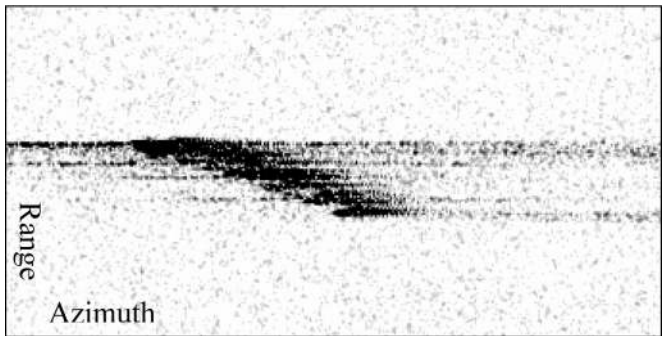

Fig. 7. Image by minimum-entropy autofocus with a fixed-order polynomial model from the simulated data.

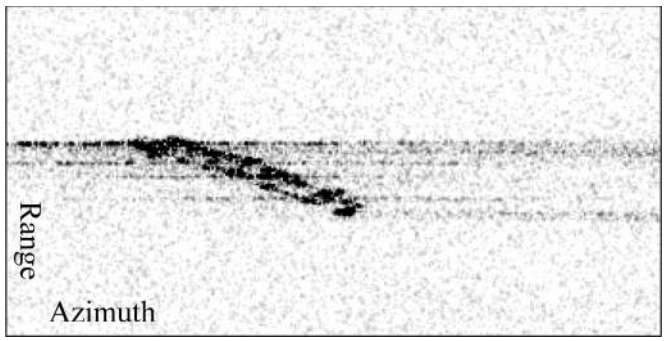

Fig. 8. Image by minimum-entropy autofocus with an adaptive-order polynomial model from the simulated data.

TABLE I
ENTROPIES OF IMAGES IN FIGS. 3–8

	Conventional Focus	Minimum-Entropy Autofocus with a Fixed-Order Polynomial Model	Minimum-Entropy Autofocus with an Adaptive-Order Polynomial Model
Original Data	-1.51062×10^{12}	-1.58211×10^{12}	-1.58307×10^{12}
Simulated Data	-1.50965×10^{12}	-1.52766×10^{12}	-1.57458×10^{12}

V. CONCLUSION

The presented minimum-entropy algorithm is effective for autofocus in SAR imaging. The phase response of the focus filter is modeled as a specially designed polynomial, and the coefficients of this polynomial are adjusted in sequence to minimize the entropy of the image. The order of this polynomial is adaptive, and thus, this algorithm applies more widely than the minimum-entropy algorithms with a fixed-order polynomial model.

ACKNOWLEDGMENT

The authors would like to thank the Technical University of Denmark for providing the data.

REFERENCES

[1] J. C. Curlander and R. N. McDonough, *Synthetic Aperture Radar: Systems and Signal Processing*. Hoboken, NJ: Wiley, 1991.
[2] R. K. Raney, H. Runge, R. Bamler, I. G. Cumming, and F. H. Wong, "Precision SAR processing using chirp scaling," *IEEE Trans. Geosci. Remote Sens.*, vol. 32, no. 4, pp. 786–799, Jul. 1994.

[3] R. Bamler, "A comparison of range-Doppler and wavenumber domain SAR focusing algorithms," *IEEE Trans. Geosci. Remote Sens.*, vol. 30, no. 4, pp. 706–713, Jul. 1992.
[4] P. H. Eichel, D. C. Ghiglia, and C. V. Jakowatz, "Speckle processing method for synthetic aperture radar phase correction," *Opt. Lett.*, vol. 14, no. 1, pp. 1–5, Jan. 1989.
[5] D. E. Wahl, P. H. Eichel, D. C. Ghiglia, and C. V. Jakowatz, "Phase gradient autofocus—A robust tool for high resolution SAR phase correction," *IEEE Trans. Aerosp. Electron. Syst.*, vol. 30, no. 3, pp. 827–835, Jul. 1994.
[6] S. Barbarossa and A. Farina, "A novel procedure for detecting and focusing moving objects with SAR based on the Wigner-Ville distribution," in *Proc. IEEE Int. Radar Conf.*, 1990, pp. 44–50.
[7] Y. G. Niho, "Phase difference auto focusing for synthetic aperture radar imaging," U.S. Patent 4 999 635, Mar. 12, 1991.
[8] E. A. Herland, "Seasat SAR processing at the Norwegian Defense Research Establishment," in *Proc. EARSeL-ESA Symp.*, 1981, pp. 247–253.
[9] R. P. Bocker, T. B. Henderson, S. A. Jones, and B. R. Frieden, "A new inverse synthetic aperture radar algorithm for translational motion compensation," *Proc. SPIE*, vol. 1569, pp. 298–310, 1991.
[10] X. Li, G. Liu, and J. Ni, "Autofocusing of ISAR images based on entropy minimization," *IEEE Trans. Aerosp. Electron. Syst.*, vol. 35, no. 4, pp. 1240–1251, Oct. 1999.
[11] D. Kasilingam, J. Wang, J. Lee, and R. Jensen, "Focusing of synthetic aperture radar images of moving targets using minimum entropy adaptive filters," in *Proc. IEEE Int. Geosci. and Remote Sens. Symp.*, 2000, pp. 74–76.
[12] J. R. Fienup and J. J. Miller, "Aberration correction by maximizing generalized sharpness metrics," *J. Opt. Soc. Amer. A, Opt. Image. Sci.*, vol. 20, no. 4, pp. 609–620, Apr. 2003.
[13] J. Wang, X. Liu, and Z. Zhou, "Minimum-entropy phase adjustment for ISAR," *Proc. Inst. Elect. Eng., Radar, Sonar Navigat.*, vol. 151, no. 4, pp. 203–209, Aug. 2004.
[14] J. Wang and X. Liu, "SAR minimum-entropy autofocus," in *Proc. Int. Radar Conf.*, 2004.